Investigating the use of Targeted-Energy-Transfer devices for stay-cable vibration mitigation

Matteo Izzi[1], Luca Caracoglia[2,*] and Salvatore Noè[1]

[1]Department of Engineering and Architecture, University of Trieste, Piazzale Europa 1, 34127, Trieste, Italy

[2]Department of Civil and Environmental Engineering, Northeastern University, 360 Huntington Avenue, Boston, Massachusetts 02115, USA

SUMMARY

Free vibrations of a taut-cable with an attached passive Targeted-Energy-Transfer (TET) device are investigated using an analytical formulation of the complex generalized eigenvalue problem. This problem is of considerable practical interest in the context of stay-cable vibration suppression in bridges, induced by wind, rain-wind and parametric excitation. The TET device is a nonlinear apparatus, which has been investigated and successfully applied to the vibration suppression in several structural or mechanical systems. This study proposes, for the first time, the use of the TET device as a simple passive apparatus for stay-cable vibration mitigation. In this application the device was modelled as a dashpot with a viscous damper in parallel with a power-law nonlinear elastic spring element and a lumped mass restrained to one end (Figure 1b). The "flexibility of the support" (imperfect anchorage to the deck) was also simulated by placing an elastic support (linear elastic spring) in series between the dashpot and the deck. The study derives a new family of "universal design curves" for the TET device, by accounting for the effects of nonlinear elastic stiffness, lumped mass and flexibility of the support. To verify the adequacy of the universal curves and to evaluate the effectiveness of the TET devices, parametric numerical simulations were performed on a reference stay-cable. As an application example, analytical results were employed to design the dampers of two flexible stays, installed on two existing cable-stayed bridges. In all the investigations, theoretical and numerical results were obtained and compared.

KEY WORDS: cable-stayed bridges, stay-cable vibration, passive control, mechanical dampers, nonlinear dynamics

[*] Corresponding author: Luca Caracoglia, Associate Professor, Department of Civil and Environmental Engineering, Northeastern University, 400 Snell Engineering Center, 360 Huntington Avenue, Boston, MA 02115, USA, tel. 617-373-5186.

E-mail addresses: matteo.izzi@phd.units.it (M. Izzi), lucac@coe.neu.edu (L. Caracoglia), noe@units.it (S. Noè)

1. INTRODUCTION

The mitigation of large-amplitude oscillation on inclined stays, associated with the effects of wind, rain-wind [1-3] and various sources of parametric excitation [4-7], has been the focus of several investigations in recent years due to the potential high costs of maintenance or repair that can be caused by, for example, fatigue in the cables. To suppress the problematic vibrations, passive damping systems have been widely studied and employed. The most common, simple to install and effective solution considers the use of a hydraulic damper placed in the proximity of the deck and connected to a stay. The taut-string theory has been traditionally employed to examine the stay-cable dynamics [8]. Analytical solution and closed-form asymptotic approximations have been developed for the taut-string problem with attached linear viscous damper, perfectly "fixed" and anchored to the deck [9-11] and for a linear viscous damper with internal stiffness [12]. Other authors have evaluated the effectiveness of the damping system by introducing the influence of the flexibility in the damper support [13] or the influence of a friction threshold in a viscous damper (e.g., [14]). The use of a hydraulic damper with nonlinear dissipation has also been proposed to increase the performance of the linear devices (e.g., [15-17]). Finally, semi-active control via magneto-rheological dampers, either attached to the deck (e.g., [18]) or incorporated into a "TMD-like" device (tuned-mass damper [19]), has also been considered to suppress the vibration.

Preferable requirements for the practical implementation of any damping device are its simplicity of installation and maintenance. Despite the technological advancements in recent years, it seems that the manufacturing, installation and long-term maintenance of a hydraulic device with prescribed nonlinear or semi-active dissipation characteristics still present some challenges.

As a result, this study explores the use of a new concept and damping device for stay-cable mitigation. The new device is a derivation of the "increasingly popular" TET (Targeted-Energy Transfer) device [20,21], a passive device with linear damping and cubic elastic restoring effect, which has gained considerable attention in various fields of engineering (mechanical, aeronautical [21] and civil [22]). This TET device would be much simpler to assemble and easy to maintain, compared to other devices above. It has been shown that a further advancement of the TET concept (the Nonlinear Tuned Vibration Absorber, or NLTVA [23]) is effective for vibration suppression in nonlinear mechanical systems as well; in particular, as demonstrated in

[23], the degree of stiffness nonlinearity (polynomial) in the NLTVA should be selected in accordance with the anticipated stiffness nonlinearity in the primary system. This would also make the TET device attractive if nonlinear geometry effects may become of concern in wind-induced stay-cable vibration (e.g., [24]).

Inspired by the recent technical advancements of TET devices and after examining the above-mentioned studies on damping devices for stay-cables, the theory of stay-cable vibration suppression is extended in this work to a generalized TET model (Figure 1b). In this model a nonlinear stiffness element, simulated by a power-law elastic spring element with generic odd exponent, is placed in parallel with a linear viscous damper and a third spring element is used to simulate the effects of an imperfect anchorage to the deck (elastic support).

The TET device, proposed in this paper, acts as a passive "sink" of unwanted vibrations, generated by external impulsive excitation [20,21] that simulates an aeroelastic loading source. In fact, it can be shown that, depending on amplitude conditions, the vibrational energy of the cable (main system) gets passively "pumped" [20] into the damping device (subsystem) in a one-way irreversible fashion. Moreover, if carefully calibrated, the TET device is able to operate on various frequencies, attracting multi-frequency transient disturbances. Depending on the environment conditions, this last aspect is of particular importance since cable oscillations may occur in the first modes of vibration; also, this mechanism seems quite interesting since it can promote the energy transfer from lower modes to higher modes of the cable [25].

The performance of a stay, equipped with the proposed device, is based on the simulation of the free-vibration dynamic cable response by including the nonlinear effects of the TET device. This approach is meaningful because the oscillations are predominantly aeroelastic and not aerodynamic, bearing in mind that the ultimate goal is to provide simple solutions for engineering design. The aim of the study was not to examine other effects, such as the response induced by wind turbulence. Also, since a unique model for the simulation of aeroelastic forces under various excitation mechanisms (e.g., rain-wind-induced vibration, dry galloping, etc.) is not available, the use of free-vibration dynamics has been often suggested as a sufficiently accurate simple method, based on systematic frequency and damping studies, to analyse and to design mitigation devices for stays.

Furthermore, in the simulations of the cable dynamics, the hypotheses of non-shallow cable, no mechanical damping and no flexural stiffness in the link elements are utilized. Even though several studies have emphasized the need for nonlinear cable dynamics simulation (e.g., [26-32]), the taut-cable theory, first introduced by Irvine [8], has been used in this study to describe the stay dynamics as this theory is usually adequate for design of dissipation devices and has been often employed by researchers (e.g. [9,10,13,15,33-36]) to analyse the motion of the system. Our experience with full-scale investigation (e.g., [37,38]) suggests that the shallow-cable effect in the long stays of a cable-stayed bridge with lengths in the range between 150 and 200 m (approximately) leads to a variation in the frequency of the symmetric extensional modes of the order of few percent only for the longest stays (and for first-mode frequency only); this approximation is also usually acceptable from the practical point of view, i.e., for the actual design of the dissipation device [2]. Preliminary results of this study can be found in [39].

This paper is organised as follows. The analytical formulation of the complex generalized eigenvalue problem for a generic TET device is presented in Section 2; under the hypothesis of small frequency shift, an asymptotic solution of the previous problem is derived in Section 3 ("universal design curves" of modal damping). A discrete model of a cable equipped with a TET device is derived in Section 4, and subsequently used to verify the adequacy of the approximate analytical solutions. The same model is also used in Section 5 to perform a parametric study of the TET device, starting from the case of the "linear hybrid TET" and extending the analysis to the general case of nonlinear TET device. Application of hybrid TET devices to a real stay is illustrated in Section 6, while discussion of the results and concluding remarks are presented in Section 7.

2. PROBLEM FORMULATION

The model for simulating the vibrations of a stay-cable with damper device is derived from basic formulations and results in this field [9,10]. The cable of length L equipped with the TET, is depicted in Figure 1a. The TET is located at a distance $x_1 = L_1$ from the left end (deck side); the cable force is T and the mass per unit length is μ. As outlined in the previous section, the dissipation mechanism in the TET device is modelled as a dashpot (Figure 1b) with viscous damping coefficient c in parallel with a power-law elastic spring with stiffness k_M and exponent n, defined as a positive and odd number ($n = 1,3...$). In order to ensure the "energy pumping" between the cable (main system) and the damper device (subsystem), a secondary lumped mass

m_A is incorporated in the apparatus at one extremity of the dashpot (Figure 1b). A linear elastic spring with stiffness k_S is also added between the dashpot and the ground to account for an imperfect anchorage of the device to the deck [13]. It must be noted that the layout of the proposed apparatus with additional spring-type connection to ground is compatible with one of the configurations comprehensively analysed in [20,21], as it ensures transfer of momentum and energy redistribution from the main system to the secondary system; more details may also be found in [20,21] and in Section 3.2. In the following analysis it is convenient to introduce the complementary coordinate $x_2 = (L - x_1)$ and the complementary length $L_2 = (L - L_1)$.

Assuming that the tension T is large compared to the weight of the stay and under the hypotheses of small vibration, negligible bending stiffness and small mechanical damping in the stay, a taut-string model is used to simulate the dynamics of the system [10]. Linear oscillations of the cable, under the assumption of virtually unchanged cable force, are described by the linear wave equation [8]:

$$\mu \frac{\partial^2 y_k(x_k,t)}{\partial t^2} = T \frac{\partial^2 y_k(x_k,t)}{\partial x_k^2}, \tag{1}$$

with $y_k(x_k,t)$ the transverse vibration and x_k the coordinate along the cable chord axis in the kth sub-string (with $k = \{1,2\}$). Equation (1) is valid everywhere except at the TET attachment point; at this location continuity of displacement and equilibrium of internal forces must be satisfied. To solve Equation (1) subjected to boundary, continuity and equilibrium conditions a non-dimensional time $\tau = \omega_{0,1} t$ (e.g., [11]) is introduced, with $\omega_{0,1} = \pi / L \sqrt{T/\mu}$ undamped natural frequency of the first native cable mode. Separation of variables is used to describe the motion over the cable segments in the form $y_k(x_k,t) = Y_k(x_k) \cdot \exp(\imath \lambda \tau)$ (e.g., [9]), with $k = \{1,2\}$, λ non-dimensional eigenvalue, $Y_k(x_k)$ complex mode shape on kth cable segment, and $\imath = \sqrt{-1}$ the imaginary unit. This substitution into Equation (1) leads to an ordinary differential equation where the solutions are the complex mode shapes of the system [9,10]. Enforcing the continuity of displacement at the TET device linkage and the boundary conditions of zero displacement at the cable end leads to $Y_k(x_k) = \gamma \cdot \sin(\pi \lambda x_k / L) / \sin(\pi \lambda L_k / L)$ (e.g., [10]), in which γ is the vibration amplitude of the cable at the TET device location, and L_k is the length of the kth cable sub-string. The equilibrium equations at node A and B (Figure 1b) for the TET device are formulated as follows:

$$-m_A \ddot{s} + k_S s - c\left(\dot{y}_{x_1=L_1} - \dot{s}\right) - k_M \left(y_{x_1=L_1} - s\right)^n = 0\,, \tag{2}$$

$$T\left(-\frac{\partial y_2}{\partial x_2}\bigg|_{x_2=L_2} - \frac{\partial y_1}{\partial x_1}\bigg|_{x_1=L_1}\right) + c\left(\dot{y}_{x_1=L_1} - \dot{s}\right) + k_M \left(y_{x_1=L_1} - s\right)^n = 0\,, \tag{3}$$

where n is positive and odd, $y_{x_1=L_1} = y_1\left(x_1 = L_1, t\right)$, the "dot" marker denotes a differentiation with respect to time t, and the variable $s(t) = s_0 \cdot \exp(\iota\lambda\tau)$ is used to represent the displacement at node A (Figure 1a). To solve these equations, an energy-based approach is adopted, in which the nonlinear force-displacement relationship of the elastic spring with stiffness k_M is reduced to a linear equivalent law (Figure 2). After this simplification, the equilibrium equations yield:

$$\sin(\pi\lambda) + \frac{1}{\pi\lambda} \cdot \frac{\left[\nu_A (\pi\lambda)^2 + \chi_S\right]\left[\eta\pi\lambda - \iota\chi_M \left(\Delta_{\tau,\sec}/L\right)^{n-1}\right]}{\eta\pi\lambda - \iota\left[\nu_A(\pi\lambda)^2 + \chi_S + \chi_M\left(\Delta_{\tau,\sec}/L\right)^{n-1}\right]} \sin\left(\pi\lambda L_1/L\right)\sin\left(\pi\lambda L_2/L\right) = 0\,, \tag{4}$$

where $\eta = c/\sqrt{\mu T}$ is the non-dimensional damper coefficient, $\chi_S = k_S L/T$ and $\chi_M = k_M L^n/T$ are the two non-dimensional spring stiffness coefficients, $\nu_A = m_A/(\mu L)$ is the non-dimensional TET mass coefficient, and $\Delta_{\tau,\sec}$ is the relative peak displacement amplitude between nodes A and B for the system characterized by the linear equivalent spring. It is interesting to note that Equation (4) is a generalized version of the equation first found in [9]. As reported in Equation (5) below, the value of $\Delta_{\tau,\sec}$ is derived from the peak vibration amplitude at the damper location $\Delta_\tau = \max\left[\left|\gamma - s_0\right|\exp(\iota\lambda\tau)\right]$ of the nonlinear system (Figure 2), through energy-based approach, by equating the elastic energy of the two systems:

$$\int_0^{\Delta_\tau} k_M x^n \mathrm{d}x = \int_0^{\Delta_{\tau,\sec}} \left(k_M \Delta_{\tau,\sec}^{n-1}\right) x \mathrm{d}x\,. \tag{5}$$

In Equation (5) the variable x represents the relative displacement between node A and B (Figure 1b); the integration of the previous equation leads to the following expression for the "secant" maximum relative vibration amplitude (linearized) as a function of the corresponding nonlinear variable:

$$\Delta_{\tau,\sec} = \sqrt[n+1]{\frac{2}{n+1}}\Delta_\tau . \tag{6}$$

3. COMPLEX EIGENFREQUENCIES AND DAMPING RATIOS FOR SMALL FREQUENCY SHIFT

3.1. General equation for complex frequency shift and TET's universal design curve

Equation (4) is also called frequency equation [9,10]. The complex roots of this equation represent the "eigenvalues" (null space) of the system, each of which corresponds to a distinct mode of vibration. Each eigenvalue λ_i can be written in terms of real and imaginary parts as $\lambda_i = \left(\omega_i / \omega_{0,1}\right)\left(\iota\zeta_i + \sqrt{1-\zeta_i^2}\right)$, where ζ_i is the damping ratio, and ω_i is the modulus of the dimensional eigenvalue [9,13].

For specific values of η, χ_S, χ_M, ν_A and L_1 / L Equation (4) can be numerically solved to a designated degree of accuracy to obtain frequencies and, most importantly, damping ratios of as many "modes" as desired (keeping in mind the approximation introduced by the linearization). Equation (4) is also based on the hypothesis that the vibration of the systems with non-linear device can still be approximately described by linear modes [15]. If the damper-induced frequency shifts are small ($L_1 / L << 1$) the complex eigenfrequencies are $\lambda_i = i + \Delta\lambda_i \cong i$, where $\Delta\lambda_i$ is the complex valued frequency shift [9]. Substituting the sinusoidal approximations $\sin\left(\pi\lambda\right) = \pi\left(-1\right)^i \Delta\lambda_i$, $\sin\left(\pi\lambda L_1 / L\right) = i\pi L_1 / L$ and $\sin\left(\pi\lambda L_2 / L\right) = \pi\left(-1\right)^i \left[\Delta\lambda_i - iL_1 / L\right]$, proposed by Krenk [9], in Equation (4) and solving for $\Delta\lambda_i$ leads to the following expression:

$$\Delta\lambda_i = i\frac{L_1}{L}\frac{\pi^2\kappa - \iota\frac{L_1}{L}\chi_M\left(\Delta_{\tau,\sec}/L\right)^{n-1}}{\pi^2\kappa\psi_{(i)} - \iota\left[1+\psi_{(i)}\frac{L_1}{L}\chi_M\left(\Delta_{\tau,\sec}/L\right)^{n-1}\right]}, \tag{7}$$

with $\psi_{(i)} = 1 + \left(L_1 / L\right)^{-1}\left\{\chi_S^{-1} + \left[\nu_A\left(i\pi\right)^2\right]^{-1}\right\}$ "generalized flexibility" of the TET apparatus, which includes the flexibility of the support $\xi = 1 + \left(\chi_S L_1 / L\right)^{-1}$ first introduced by Huang and Jones [13]. The designation "generalized flexibility" is used in this context to indicate the ability of the device to deform (through the spring attachment) or transfer momentum (through the secondary TET mass). The flexibility term is mode dependent with $i = \{1, 2, ...\}$ due to the effect of the secondary TET mass, which influences the energy pumping mechanism. For small masses and low-order modes it can be approximately assumed that the variation $\psi(i)$ is small compared to other terms, since the effect of χ_S^{-1} is dominant compared to $\left[\nu_A (i\pi)^2\right]^{-1}$. For $0 < \nu_A < 0.005$ the second term can be neglected, leading to an approximate formulation (still acceptable, as later shown in the example)with $\psi_{(i)} \approx \psi \approx \xi$ similar to the formulation proposed by Huang and Jones [13].

As shown at the beginning of this subsection, the imaginary part of the eigenfrequencies λ_i represents the attenuation due to damping. Under the hypothesis of small damper-induced frequency shifts, the modal damping ratio ζ_i in a given mode $i = \{1, 2, ...\}$ can be calculated as $\zeta_i = \mathrm{Im}[\lambda_i]/|\lambda_i| \cong \mathrm{Im}[\lambda_i]/i$ [9]. Using this approximation along with the solution of $\mathrm{Im}[\lambda_i]$ (imaginary part of the root) leads to the following approximate formula of the normalized modal damping ratios $\zeta_i/(L_1/L)$:

$$\frac{\zeta_i}{L_1/L} \cong \frac{\pi^2\kappa}{\left[\pi^2\kappa\psi_{(i)}\right]^2 + \left[1 + \psi_{(i)}(L_1/L)\chi_M\left(\Delta_{\tau,\sec}/L\right)^{n-1}\right]^2}, \tag{8}$$

where $\kappa = i\eta/\pi(L_1/L)$ is a non-dimensional parameter group, referred to as the normalized damper coefficient [10] in the following sections. Equation (8) is also labelled as the "universal design curve" [11] of the modal damping ratio versus normalized damper coefficient κ. The non-dimensional parameter group κ varies between zero and infinity. If $\kappa = 0$ the system is undamped and the cable is attached to an elastic device made of two elastic springs arranged in series, respectively χ_S and χ_M, with the TET mass interposed among them. If $\kappa \to \infty$ the damper is perfectly clamped to the stay, the elongation between node A and B tends to zero with no dissipation and cable vibration controlled by the flexibility χ_S^{-1}.

3.2. Considerations on energy pumping mechanism and dual-modality dissipation of the TET

As shown in Equation (8), the flexibility of the TET apparatus is a function of the non-dimensional TET mass coefficient ν_A, the dimensionless stiffness of the support χ_S. A predefined value of $\psi_{(i)}$ may always be found by appropriately combining the values of the two parameters.

If $\psi_{(i)} \to 1$ the TET device is rigidly restrained to ground in correspondence of node A; this limit coincides with the condition that either ν_A or χ_S must tend to infinity. In this case the TET device is reduced to a dashpot composed of a linear viscous damper in parallel with a power-law nonlinear elastic spring element connected to a rigid support.

If $\psi_{(i)}$ is greater than one, three regimes are possible. If both ν_A and χ_S have a finite non-zero value the mechanical apparatus is analogous to the one depicted in Figure 1b. Since the mass of the subsystem is usually quite small compared to the main system in real applications ($0 < \nu_A \leq 0.05$), the device must be weakly coupled to the ground ("compliant support") to enhance the energy pumping mechanism. In this regime the apparatus behaves like a "Configuration-I" TET device according to the classification by Vakakis *et al*. [21] and, as described in the previous section, the performance is mode dependent due to the effect of the TET mass in the flexibility $\psi_{(i)}$. On the contrary, if the device is strongly coupled to the ground (relevant stiffness of the support with large χ_S), the effect of the secondary mass can be neglected (as if it were $\nu_A \to 0$) and the energy pumping is less likely to be activated. In this second scenario the apparatus behaves like a passive dashpot on an elastic support.

Finally, if the elastic stiffness of the support $\chi_S \to 0$ there is no connection between the deck and the device and the mechanical apparatus acts like a "Configuration-II" TET device [21], also referred to as Nonlinear Energy Sink (NES). The NES apparatus has a strongly nonlinear behaviour and might be installed in any position along the cable length. Nevertheless, the use of the universal design curve to predict the performance is only applicable if the device is installed near the cable anchorage. The performance of this device is usually worse compared to the one of the Configuration-I device [21] due to a generally higher $\psi_{(i)}$ for the same values of ν_A, even though it might be capable to absorb and dissipate energy by transient resonance captures [21] for a wider spectrum of frequencies. The various regimes will be described in a later section.

3.3. Optimal design point of the TET

The optimal damping ratio can be derived from Equation (8) by setting the derivative with respect to κ equal to zero; this gives:

$$\kappa_{\text{opt}} = \frac{1}{\left[\pi\psi_{(i)}\right]^2}\left[1+\psi_{(i)}\left(L_1/L\right)\chi_M\left(\Delta_{\tau,\text{sec}}/L\right)^{n-1}\right], \tag{9}$$

and the corresponding "optimal damping ratio" [10] can be written as:

$$\frac{\zeta_{i,\text{opt}}}{L_1/L} = \frac{1}{2\psi_{(i)}\left[1+\psi_{(i)}\left(L_1/L\right)\chi_M\left(\Delta_{\tau,\text{sec}}/L\right)^{n-1}\right]}. \tag{10}$$

Equation (10) shows that the optimal damping ratio of a TET device is amplitude dependent as long as n is greater than one, while there is no relationship between the peak displacement amplitude at the TET device linkage and the damping ratio if n is equal to one (Linear TET device). Since κ is proportional to the mode number i, the optimal damping ratio can usually be achieved in one mode at a time (which is also common in linear devices, e.g., [10]). In particular, if the TET device is designed optimally for a particular mode, it will be more "rigid" in the higher modes and less "compliant" in the lower modes, showing moderately suboptimal damping ratios in both situations.

4. FORMULATION OF THE EQUALLY-SPACED LUMPED MASS MODEL

A second numerical model has been used to evaluate the effectiveness of the TET devices (linear and nonlinear) and the simplified solution by linearization (e.g., Equation (8)). This model is a time-domain lumped-mass model of a stay, equipped with the TET device. In the cable model n' concentrated masses, equally spaced at a distance Δx (simulating the distributed mass of the stay μ) are linked by massless cable elements, axially loaded by a constant internal force T (Figure 3a). Each discrete degree of freedom in the transverse direction, $y_i = y_i(t)$, is associated with each concentrated mass $M_i = \mu \cdot \Delta x$ [40]. An additional degree of freedom $j_A = n'+1$ and a mass m_A are employed to simulate the behaviour of the lumped TET mass, restrained at the bottom of the TET device, and the flexibility of the support. The degree of freedom of the cable to which the TET device is attached (node B, Figure 1b) is defined as j_B. For compatibility with Equation (1), hypotheses of non-shallow cable, no mechanical damping, and no flexural stiffness in the link elements are used. From the free-body equilibrium diagram (Figure 3b) of each nonrestrained mass element of the taut-cable (inertial forces and effect of cable tension T, simulated by transverse forces F_L "left" and F_R "right") the dynamic equilibrium equation is:

$$M_i \ddot{y}_i - T/\Delta x\left(y_{i-1} - 2y_i + y_{i+1}\right) = 0, \tag{11}$$

being $\ddot{y}_i = \mathrm{d}^2 y_i/\mathrm{d}t^2$, with $i = 1 \ldots n'$ and $i \neq j_B$. Two additional equilibrium equations are introduced at the j_B and j_A degrees of freedom to locally characterize the TET device:

$$M_{j_B}\ddot{y}_{j_B} - T/\Delta x\left(y_{j_B-1} - 2y_{j_B} + y_{j_B+1}\right) = -f_{j_B}, \quad m_A \ddot{y}_{j_A} + k_{j_A} y_{j_A} = f_{j_B}; \tag{12-13}$$

where $f_{j_B} = c\left(\dot{y}_{j_B} - \dot{y}_{j_A}\right) + k_M\left(y_{j_B} - y_{j_A}\right)^n$ is the interaction force provided by the dashpot, with $\dot{y}_i = \mathrm{d}y_i/\mathrm{d}t$. The matrix form of the dynamical system is:

$$\mathbf{M}\ddot{\mathbf{y}}(t) + \mathbf{K}\mathbf{y}(t) = \mathbf{f}(t) \tag{14}$$

with $\mathbf{y}(t)$ and $\ddot{\mathbf{y}}(t)$ column vectors of the transverse displacements and accelerations, and $\mathbf{M}$ and $\mathbf{K}$ mass and stiffness matrices of the cable and elastic support, assembled as:

$$\mathbf{M} = \begin{bmatrix} \mathbf{M}_{\text{cable}} & \mathbf{0}_{(n'\times 1)} \\ \mathbf{0}_{(1\times n')} & m_A \end{bmatrix}, \quad \mathbf{K} = \begin{bmatrix} -\dfrac{T}{\Delta x}\mathbf{K}_1 & \mathbf{0}_{(n'\times 1)} \\ \mathbf{0}_{(1\times n')} & k_S \end{bmatrix}, \quad \mathbf{K}_1 = \begin{bmatrix} -2 & 1 & 0 & \cdots & 0 \\ 1 & \ddots & \ddots & \ddots & \vdots \\ 0 & \ddots & \ddots & \ddots & 0 \\ \vdots & \ddots & \ddots & \ddots & 1 \\ 0 & \cdots & 0 & 1 & -2 \end{bmatrix}; \tag{15-17}$$

in which $\mathbf{M}_{\text{cable}} = \mu \cdot \Delta x \cdot \mathbf{I}_{n'\times n'}$ is the lumped mass matrix of the cable, and $\mathbf{K}_1$ in Equation (17) is an $n' \times n'$ indicator-matrix of zeros, ones and minus twos. In Equation (14) $\mathbf{f}(t)$ is the column vector of external "forcing" functions, in which the only two non-zero elements collect the actual forces transmitted between the TET device and the stay (degrees of freedom j_A and j_B). The following non-dimensional dynamic system is later obtained, with non-dimensional transverse displacements $z_i(t) = y_i(t)/L$, non-dimensional time $\tau = \omega_{0,1}t$, $\mathrm{d}z_i/\mathrm{d}t = \omega_{0,1}\left(\mathrm{d}z_i/\mathrm{d}\tau\right)$ and $\mathrm{d}^2 z_i/\mathrm{d}t^2 = \omega_{0,1}^2\left(\mathrm{d}^2 z_i/\mathrm{d}\tau^2\right)$:

$$\frac{\mathrm{d}^2\mathbf{z}(\tau)}{\mathrm{d}\tau^2} + \mathbf{K}_{\text{nd}}\mathbf{z}(\tau) = \mathbf{f}_{\text{nd}}(\tau), \quad \mathbf{K}_{\text{nd}} = \frac{1}{\omega_{0,1}^2}\mathbf{M}^{-1}\mathbf{K} = \begin{bmatrix} -\dfrac{N_{\text{d}}^2}{\pi^2}\mathbf{K}_1 & \mathbf{0}_{(n'\times 1)} \\ \mathbf{0}_{(1\times n')} & \dfrac{\mu\cdot\Delta x}{m_A}\dfrac{N_{\text{d}}}{\pi^2}\chi_S \end{bmatrix}, \tag{18-19}$$

where vector $\mathbf{z}(\tau)$ collects all z_i terms, while $N_\mathrm{d} = L/\Delta x$ is a scalar parameter. The only two non-zero elements of the non-dimensional vector $\mathbf{f}_\mathrm{nd}(\tau) = \omega_{0,1}^{-2} \cdot \mathbf{M}^{-1} \cdot \mathbf{f}(\tau)$ are, respectively:

$$\mathrm{f}_{\mathrm{nd}_{j_B}}(\tau) = -\frac{N_\mathrm{d}}{\pi}\left\{\eta\left[\frac{\mathrm{d}\,z_{j_B}}{\mathrm{d}\tau} - \frac{\mathrm{d}\,z_{j_A}}{\mathrm{d}\tau}\right] - \frac{\chi_M}{\pi}\left[z_{j_B} - z_{j_A}\right]^n\right\}, \quad \mathrm{f}_{\mathrm{nd}_{j_A}}(\tau) = -\frac{\mu\Delta x}{m_A}\mathrm{f}_{\mathrm{nd}_{j_B}}(\tau) \quad (20\text{-}21)$$

To solve the nonlinear dynamic problem of Equation (18), $\mathbf{z}$ is recast in state-space form as $\mathbf{w} = \{\mathbf{z}, \mathrm{d}\mathbf{z}/\mathrm{d}\tau\}^T$, with $\mathrm{d}\mathbf{w}/\mathrm{d}\tau = \{\mathrm{d}\mathbf{z}/\mathrm{d}\tau, \mathrm{d}^2\mathbf{z}/\mathrm{d}\tau^2\}^T$ and $\{\cdot\}^T$ denoting transpose operator. This leads to a state-space linear system of $(2n'+2)$ equations with $\mathbf{f}^* = \{\mathbf{0}_{((n'+1)\times 1)}, \mathbf{f}_\mathrm{nd}\}^T$:

$$\frac{\mathrm{d}\mathbf{w}}{\mathrm{d}\tau} = \mathbf{S}\mathbf{w} + \mathbf{f}^*, \qquad \mathbf{S} = \begin{bmatrix} \mathbf{0}_{(n'+1)\times(n'+1)} & \mathbf{I}_{(n'+1)\times(n'+1)} \\ -\mathbf{K}_\mathrm{nd} & \mathbf{0}_{(n'+1)\times(n'+1)} \end{bmatrix}, \qquad (22, 23)$$

The vibration response of the discrete nonlinear dynamic system of Equation (22) is numerically solved, with zero initial conditions $\mathbf{w}(\tau = 0) = \mathbf{0}_{(2n'+2)\times 1}$, by means of a fourth-order Runge-Kutta integration algorithm. At the beginning of each simulation, the system is subjected to an initial transitory forced-vibration phase, in which a set of concentrated harmonic forces, suitably placed at selected degrees of freedom, is applied to excite the cable motion in one specific mode. After this initial phase the forces are removed and the free-vibration response is analysed. Modal damping ratio, supplied through the TET device, is evaluated by applying the logarithmic decrement method [41] to the motion of a reference degree of freedom, relevant to the dynamics of the entire system.

5. NUMERICAL SIMULATIONS

Parametric numerical simulations investigate the free-vibration response of the first five modes of a prototype reference stay, composed of a 20m-long stay-cable with $T = 1900\mathrm{kN}$, diameter $D = 0.14\mathrm{m}$, $\mu = 47.9\mathrm{kg/m}$, and a TET device located near an anchorage.

The first set of simulations have been performed with a hybrid formulation of the mechanical apparatus discussed in the previous sections (Hybrid TET, H-TET), in which the effects of the TET mass m_A are negligible ($m_A \ll \mu L$ and $\psi_{(i)} \approx \xi$). The hybrid formulation is used to investigate the effects of the elastic stiffness k_M in parallel with the viscous damper. Two types of H-TET are examined: a Linear device (H-L-TET) characterized by $n = 1$, and a Nonlinear device (H-NL-TET) with $n = 3$. Five different flexibility coefficients ξ have been considered to realistically simulate the support conditions [13].

The second set of analyses investigated the general formulation of the TET considering a mass m_A sufficiently large to activate the "energy pumping". Within this second set of simulations, a nonlinear cubic elastic spring element ($n = 3$) has been examined and two configurations have been investigated: the case of an apparatus weakly coupled to the deck and the NES configuration with the device uncoupled from the ground.

5.1. Hybrid Linear Targeted-Energy-Transfer device (H-L-TET)

The H-L-TET device under investigation is placed at $L_1 / L = 0.02$, with $\chi_M = 10$ and exponent $n = 1$; for each mode analysed, the peak oscillation of the cable Δ at the end of the transitory forced-vibration phase is three times the diameter of the stay ($\Delta / L = 0.02$). As mentioned before, if n is equal to one (linear device) there is no dependence of the damping ratio on the peak displacement amplitude at the H-L-TET device linkage (Equation (8)). Figure 4a shows the normalized damping ratio $\zeta_i / (L_1 / L)$ versus the normalized damper coefficient κ for the first five modes of the reference cable and for five flexibility coefficients ξ ($\xi = 1$: rigid support to ground, $\xi = 5$: "flexible" or imperfect support). A distinct curve is plotted for each mode. The quantity $\psi_{(i)}$ is independent of the mode and it is $\psi_{(i)} = \xi$. The universal design curves (thick lines of various line types without marker), obtained from Equation (8), agree very well with the curves generated by numerical integration (thin continuous lines with marker). Equation (8) has been subsequently used, for specific values of the flexibility of the support ξ, to exploit the effects of the linear stiffness χ_M on the performances of the H-L-TET device. Figure (4b) shows the universal curves obtained with $\xi = 1.2$ and with χ_M varying between zero (linear damper with no spring in parallel) and fifty; a circle marker is used to label the local maxima, achieving optimal damping ratios. The range of χ_M has been derived from values typically used for the design of such devices (e.g., [13]). An increase in the elastic stiffness χ_M yields a reduction of both the optimal damping ratio and the slope of the curve in the proximity of the optimal-damping points, by “flattening” the bell-shaped curve in the interval of κ at which the highest damping ratios are achieved.

5.2. Hybrid Nonlinear Targeted-Energy-Transfer device (H-NL-TET)

The following analyses describe a parametric study to evaluate the behaviour and the effectiveness of the H-NL-TET devices on cable vibrations suppression. Since wind and wind-rain induced vibration can cause peak oscillations (Δ) between one and three times the diameter of the stay in the first cable modes [42], the device used to perform the analyses is optimized for the second mode of the reference cable by considering two peak displacement amplitudes belonging to the range previously mentioned. As suggested in [20,21], the H-NL-TET device analysed in this chapter is characterized by $n = 3$. In fact, it would be possible to physically build a cubic spring in a very simple way by exploiting stiffness nonlinearity influenced by change in geometric configuration of a flexible element with negligible bending stiffness (as shown in a number of prototype units, manufactured and tested in [21]). Moreover, as outlined in the introduction, if large-amplitude cable vibration is anticipated, the optimal order of the polynomial used in the nonlinear spring element of the TET device should be tuned in accordance with the “order” of geometric nonlinearity in the primary system [23].

Figure 5 shows the normalized damping ratio $\zeta_i / (L_1 / L)$ versus the normalized damper coefficient κ for a H-NL-TET placed at $L_1 / L = 0.02$ (Figures 5a-5b) and $L_1 / L = 0.04$ (Figures 5c-5d-5e-5f) when the non-dimensional elastic stiffness parameters are $\chi_M = 1.5\text{e}+05$ (Figures 5a-5c-5e) and $\chi_M = 2.0\text{e}+06$ (Figures 5b-5d-5f), and the peak displacement of the cable, normalized with respect to the cable length, is $\Delta / L = 0.01$ (Figures 5a-5b-5c-5d, about one stay diameter) and $\Delta / L = 0.02$ (Figures 5e-5f, about three stay diameters). In Figures 5a-5b with $L_1 / L = 0.02$ the curves (thin continuous lines with marker), numerically generated by lumped-mass model and corresponding to each of the first five modes of the cable agree very well with the analytically-derived universal design curves (thick lines of various line types without marker). For $L_1 / L = 0.04$ the lumped-mass-model numerical curves (Figures 5c-5d-5e-5f) are affected by a larger frequency shift than those of the previous case (neglected by the universal curve [9,10]). Numerical results agree somewhat less well with the asymptotic analytical solution, especially around the points achieving optimal damping ratio. Differences are, however, still acceptable (less than 5% in terms of damping ratio).

The results reveal that, for a fixed value of the peak vibration amplitude Δ / L, an increase in the elastic stiffness χ_M yields a reduction of both the optimal damping ratio and the slope of the curve in the proximity of the optimal-damping points (Figures 5a and 5b; Figures 5c and 5d; Figures 5e and 5f). These effects produce a "flattening" in the bell-shaped curve in the interval of κ at which the highest damping ratios are achieved. An analogous reduction is also visible when the elastic stiffness χ_M is kept constant while the peak oscillation Δ / L is increased from 0.01 to 0.02 (Figures 5c and 5e; Figures 5d and 5f). In this second situation the reduction is slightly lower than before and it is due to an increase of the elastic force within the damping device, associated with the effects of the nonlinearity, which reduces the damping proprieties and transfers the motion to the elastic support.

It must be noted that the damping ratios, shown in Figure 5, are normalized with respect to the device position along the cable's length. For this reason [9,10] the damping ratios ζ in Figures 5c-5d-5e-5f have doubled in comparison with those in Figures 5a-5b. The results also reveal that the damping ratio is predominantly influenced by the flexibility of the support, compared to the elastic stiffness in parallel with the linear viscous damper. For instance, doubling the flexibility of the support from $\xi = 1.0$ to $\xi = 2.0$ causes a 40% reduction of damping ratios while increasing more than ten times the elastic stiffness leads to a reduction lower than 5%.

The universal design curves of Figure 5 (thick lines of various line style without marker) have been obtained from Equation (8) by defining, for each analysed case, a reference value of $\Delta_{\tau,\sec}$. As shown in Equation (6), the peak vibration amplitudes Δ_τ of the nonlinear system must be first estimated and later converted to equivalent "secant" vibration amplitude $\Delta_{\tau,\sec}$ of the linearized system in order to be used in Equation (8). Therefore, a set of "reference curves", assessing the peak displacement amplitude Δ_τ of the non-linear system in the section of the damper, must be determined *a priori*. Figure 6a shows an example of the reference "abacus" curves for the device simulated in Figure 5e. First, the relationship between Δ_τ and the non-dimensional parameter group κ is established by numerical simulations (thin continuous lines with marker), repeated for the first five modes of the cable as a function of flexibility ξ; inspection of the simulations has revealed that lumped-mass-model numerical curves tend to overlap (at the same ξ with $L_1 / L << 1$ and $\Delta / L << 1$). Second, the "reference curves" (thick lines of various line types without marker), independent of the mode, are obtained for a given ξ from the five numerical simulations by means of the least-squares method.

It must be noted that the shape of the curves presented in Figure 6a depends on several factors, such as the peak vibration amplitude of the cable, the cross-section at which the TET device is installed, the non-dimensional nonlinear elastic stiffness parameter χ_M, the flexibility of the support ξ and the normalized damper coefficient κ. In order to calculate the exact values of the universal design curves (e.g., Figure 5e) it is important to identify the shape of the reference curve by preliminary simulation using the lumped-mass model (Figure 6a). Since this kind of approach is time-consuming and it is not practical for design when combined with the universal design curves, a simplified approach has been preferred. A "conservative" set of universal design curves can be estimated for the H-NL-TET by using a constant value of the peak amplitude $\Delta_{\tau,\sec}$, obtained for the undamped system with $\kappa = 0$ and irrespective of the actual relationship Δ_τ vs. κ (e.g., Figure 6a). The resulting curves, related to the device described in Figure 5e, are plotted in Figure 6b. In comparison with the results of Figure 5e, the damping ratios are lower near the optimal damping point (with maximum reduction of the order of 10%); however, negligible differences are observed everywhere else in comparison with the "exact" solution. A simplified abacus has also been proposed to predict the peak amplitude displacement of the undamped system in the section of the TET device; Figure 7 shows the results achieved for a device placed at $L_1 / L = 0.02$, when the optimal mode is the second one and the peak vibration amplitude of the cable is, respectively, $\Delta / L = 0.03$ (red line) and $\Delta / L = 0.02$ (blue line). The curves have been obtained by combining the results of the first five modes by least squares (thin continuous lines with markers) and can be used to find the conservative universal design curves, previously mentioned.

5.3. Targeted-Energy-Transfer device with $\nu_A \neq 0$

The performance of a generalised apparatus configuration, derived from the case in Figure 5f, is examined. This study aims at highlighting the differences between a hybrid and a general TET device by taking into account the effect of the secondary TET mass m_A.

The first set of simulations considers an apparatus connected to the deck with $n = 3$, $\chi_M = 2.0\text{e}{+}06$, $L_1 / L = 0.04$ and $\Delta / L = 0.02$ by studying the influence of the non-dimensional lumped mass parameter, with $\nu_A = 0.03$ (3% of cable mass, Figure 8a) and $\nu_A = 0.05$ (5% of cable mass, Figure 8b). The analyses have been performed by considering the same flexibility coefficients ξ used in Figure 5f. In order to enable the comparison with the previous results, the universal design curves shown in Figure 8a and Figure 8b have been obtained from Equation (8) by neglecting the contribution of the mass m_A ($\nu_A \approx 0$ and $\psi_{(i)}$ independent of the mode number) , whereas the contribution of the mass is included in the numerical simulations by lumped-mass model. For $\xi < 5$, the lumped-mass-model curves (thin continuous lines with marker) have negligible differences with the analogous results of Figure 5f. For $\xi = 5$ the damping ratios provided by the device are generally quite low, suggesting that the device is not suitable to mitigate the oscillations. In all the simulations, the energy pumping mechanism appears to be partially enabled only. Even though the lumped-mass-model results are affected by a non-negligible frequency shift between the undamped case and the damped one, the asymptotic solution obtained with $\nu_A \approx 0$ and $\psi_{(i)} \approx \xi$ is still acceptable (the differences are lower than 5% in terms of damping ratio).

The second set of simulations has been performed on a NES apparatus (Section 3.2), i.e., a device completely detached from the bridge deck. The setup used in the analyses is analogous to the one used in the previous set: $n = 3$, $\chi_M = 2.0\text{e}{+}06$, $L_1 / L = 0.04$ and $\Delta / L = 0.02$. Two non-dimensional TET mass configurations have been investigated, $\nu_A = 0.03$ (Figure 8c) and $\nu_A = 0.05$ (Figure 8d). In both situations, the universal design curves (thick lines without marker) obtained from Equation (8) agree quite well with the lumped-mass-model numerical curves (thin continuous lines with marker) of the second mode. However, there are significant differences in all the other modes. The performances are generally lower compared to the results depicted in Figures 5f and 8a-b, and are strongly influenced by the mode analysed and by the value of the TET mass m_A. For example, the fifth-mode damping of the numerical curve in Figure 8d is doubled compared to the analogous curve of Figure 8c. The high peaks, observable in the lumped-mass-model numerical curves of the third and fourth mode (Figure 8d), are more clearly associated with energy pumping, even though it could not be noted in any other configuration.

6. SIMULATED APPLICATION OF THE H-TET DEVICES

Numerical simulations have been carried out to investigate the performance of the device on stay AS16 of the Fred Hartman Bridge (Houston, Texas, USA). Since the performance of the TET apparatus with a consistent value of the secondary TET mass m_A have shown limited differences compared to the analogous hybrid configuration, in the following application examples the latter configuration with $\nu_A = 0.001$ has been considered .

The Fred Hartman Bridge is a twin-deck, cable-stayed bridge over the Houston Ship Channel; it has a central span of 380m and two side spans of 147m; the deck is composed of precast concrete slabs on steel girders, carried by a total of 192 cables, spaced at 15-m intervals in four inclined planes. The stay under evaluation is an 87m-long cable with $T = 2260\text{kN}$, $\mu = 47.9\text{kg/m}$ and $D = 0.141\text{m}$ [1]. The first-mode frequency of AS16 is equal to 1.24 Hz; damping ratio of the order of 0.4% was noted in the absence of damping device on this cable [37]. This stay was selected in this study since a passive viscous damping device is actually installed on the full-scale system. In contrast, other and longer cables are equipped with both cross-ties and dampers to reduce vibration [38], making a direct comparison not directly possible. More information on the cable properties including indication of supplementary devices may be found in [37].

In order to evaluate the effectiveness and the applicability of the TET device in relation to the mitigation of wind and rain-wind induced phenomena, the criterion based on the Scruton number of the cable is utilized [1,43,44]. The Scruton number S_c and the criterion are defined as $S_c = \mu\zeta_i / \left(\rho D^2\right) > 10$ where ρ is the air density (standard value $\rho = 1.225\ \text{kg/m}^3$) and ζ_i is the structural damping ratio, provided by the external damping device, of the mode being investigated [43,44]. As suggested by FHWA and PTI [1,44], since the inherent mechanical damping in the cables is extremely low (e.g., [2]) the condition $S_c > 10$ can only be satisfied if an external damping device is installed. A second criterion has alternatively been used (e.g., in Japan [45]): $\hat{S}_c = 2\mu\delta_i / \left(\rho D^2\right) > 40$, where $\delta_i \approx 2\pi\zeta_i$ is the logarithmic decrement of the structural damping for a lightly damped system. In the following comparisons the more conservative criterion $S_c = \mu\zeta_i / \left(\rho D^2\right) > 10$ has been adopted.

The H-NL-TET devices is designed to achieve the best performance in the fundamental mode of vibration and in the second one, which should still provide adequate damping to suppress wind and rain-wind induced vibration in several of the higher modes. The peak displacement amplitude in the section of the damper, used to design the optimal damper coefficient, has been obtained considering a peak vibration amplitude of the cable equal to $\Delta / L = 0.02$, measured in the anti-nodal cable section and observed in the mode designed for optimal damping. Mechanical damping of the stay and negative aerodynamic damping in the case of aeroelastic vibration are not included in the calculation of the minimum damping ratio needed to satisfy the Scruton number criterion [37].

The H-NL-TET device is placed at $L_1 / L = 0.045$ with $\chi_M = 2.0\text{e+}05$ and exponent $n = 3$. The first eight modes of the cable and four different flexibility coefficients $\xi = \{1.0, 1.2, 1.5, 2.0\}$ have been examined since these are predominantly excited by wind, as documented by full-scale investigation [37]. Figure 9a shows the modal damping ratios provided by the H-NL-TET when the optimal performance is achieved in the fundamental mode of vibration while Figure 9b depicts analogous results obtained when the damping device is designed to be optimal in the second mode. The lumped-mass-model numerical curves (thin continuous lines with marker), corresponding to each of the five modes of the cable, agree quite well with the universal design curves (thick lines of various line types without marker); a thick dotted line is used to define the minimum threshold given by the condition $S_c = 10$. As depicted in Figure 9a, for a H-NL-TET device with $\xi = 2.0$ the Scruton number criterion is satisfied in the first three modes only, while it appears inadequate for the higher modes and for larger flexibility in the support. It is important to note that the criterion based on the Scruton number is usually valid for the first few modes of vibration while its applicability to higher ones is less acceptable, and smaller values of damping ratio supplied in this last case might be adequate to mitigate the vibrations due to aeroelastic phenomena [43]. Analogous considerations are applicable to the results shown in Figure 9b, in which the optimal damping ratio is achieved in the second mode of the cable. In this second figure the Scruton criterion is satisfied in all the simulations; the TET device under evaluation appears more "rigid" in the higher modes and less "compliant" in the lower modes, showing suboptimal damping ratios in both cases.

Figure 9 suggests that the performance of the TET device is influenced by the relative distance between the installation point on the stay and the nearest anti-nodal cable section, mode by mode. This behaviour has negligible effects in the first modes (modes 1 to 5 in Figure 9), whereas it becomes relevant for the higher ones. In particular, after reaching the lowest performance around the sixth mode, the damping ratios provided by the TET device and calculated by lumped-mass model improve in the subsequent modes. It must be noted that the damping ratios predicted by the analytical formulation are always lower than the exact value obtained from the lumped-mass model; this behaviour is due to the approximation introduced to estimate the universal design curves. Nevertheless, lower damping values are acceptable from the design standpoint; the universal design curves can still be used since they provide a safe estimation, useful for practical design.

7. CONCLUSIONS

The use of new passive damper device, inspired by the Nonlinear Targeted-Energy-Transfer (TET) device, was examined for mitigating stay-cable vibrations. A new family of "universal design curves" has been found analytically, and numerically verified on a reference stay by a time-domain lumped-mass model and through a prototype application on a cable-stayed bridge.

The original aspects and main conclusions of this study are:

1) A new passive damping device is proposed and developed for stay-cable vibration mitigation, induced by wind or rain-wind. The device is derived from the TET device, recently investigated for reducing vibrations in mechanical and dynamical systems.
2) The main advantage of the TET device is the fact that the peak region of the universal amplitude-dependent damping curve is usually wider (or flatter) than the corresponding universal curve of a viscous damper. As a result, the device has a broader operational range of high damping. The control of more modes at the same time, for example through

the empirical procedure suggested by Weber *et al.* [46], can be achieved with a smaller dashpot and without a more sophisticated apparatus.

3) A new class of generalized "universal design curves", which could be employed for design of the new device, is derived analytically.
4) The new apparatus is applied to improve damping of two existing stays. The paper shows that the damping ratios of a passive device, installed very close to the anchorage, can still satisfy the Scruton number criterion even for very long cables (more than 200 meters long). It is also suggested that the use of semi-active damping, such as magneto-rheological dampers with negative stiffness (e.g., [47-49]), which has been usually preferred in these extreme situations, may not be the only practical solution.

Future studies will possibly examine the performance of the device in comparison with similar passive damping devices and analyse the behaviour of cable-damper systems under aeroelastic vibrations.

ACKNOWLEDGEMENTS

Luca Caracoglia would like to acknowledge the partial support of Northeastern University, Office of the Provost, "Tier-1 Seed Grant" for Interdisciplinary Research Projects in 2011-2014; the collaboration of Dr. Bernardo Barbiellini in the Department of Physics of Northeastern University, co-Principal Investigator of the Tier-1 project, is also gratefully acknowledged. This study was also completed while Luca Caracoglia was on sabbatical leave at the University of Trento, Italy in 2014; the support of the University of Trento's Research Fellowship program is also acknowledged.

REFERENCES

1. Bosch HR. *Wind induced vibration of stay cables*, Publication No. FHWA-HRT-05-084, US Department of Transportation, Federal Highway Administration: McLean, Virginia, USA 2007.
2. Xu Y-L. *Wind effects on cable-supported bridges*. John Wiley and Sons: Singapore, 2013.
3. Zhou HJ, Xu YL. Wind–rain-induced vibration and control of stay cables in a cable-stayed bridge. *Structural Control and Health Monitoring* 2007; **14(7):** 1013-1033.
4. Gattulli V, Lepidi M. Nonlinear interactions in the planar dynamics of cable-stayed beam. *International Journal of Solids and Structures* 2003; **40(18):** 4729-4748.

5. Gattulli V, Lepidi M. Localization and veering in the dynamics of cable-stayed bridges. *Computers & Structures* 2007; **85(21-22):** 1661-1678.

6. Liu M, Zuo D, Jones N. Analytical and Numerical Study of Deck-Stay Interaction in a Cable-Stayed Bridge in the Context of Field Observations. *Journal of Engineering Mechanics* 2013; **139(11):** 1636-1652.

7. Liu M-Y, Zuo D, Jones NP. Deck-induced stay cable vibrations: Field observations and analytical model, *Proceedings of the 6th International Symposium on Cable Dynamics*, Charleston, South Carolina, USA, 2005; 175-182.

8. Irvine HM. *Cable structures*. MIT Press: Cambridge, Massachusetts, USA, 1981.

9. Krenk S. Vibrations of a taut cable with external damper. *Journal of Applied Mechanics, ASME* 2000; **67(4):** 772-776.

10. Main JA, Jones NP. Free vibrations of a taut cable with attached damper. I: Linear viscous damper. *Journal of Engineering Mechanics, ASCE* 2002; **128(10):** 1062-1071.

11. Pacheco BM, Fujino Y, Sulekh A. Estimation curve for modal damping in stay cables with viscous damper. *Journal of Structural Engineering* 1993; **119(6):** 1961-1979.

12. Sun L, Shi C, Zhou H, Cheng W. A full-scale experiment on vibration mitigation of stay cable, *Proceedings of the IABSE Symposium Report*, 2004; 31-36.

13. Huang Z, Jones NP. Damping of taut-cable systems: effects of linear elastic spring support. *Journal of Engineering Mechanics* 2011; **137(7):** 512-518.

14. Main JA, Jones NP. Analytical investigation of the performance of a damper with a friction threshold for stay-cable vibration suppression, *Proceedings of the 15th ASCE Engineering Mechanics Conference*, Columbia University, New York, NY, USA, 2002; CD-ROM.

15. Main JA, Jones NP. Free vibrations of a taut cable with attached damper. II: Nonlinear damper. *Journal of Engineering Mechanics, ASCE* 2002; **128(10):** 1072-1081.

16. Yu Z, Xu YL. Non-linear vibration of cable-damper systems Part I: Formulation. *Journal of Sound and Vibration* 1999; **225(3):** 447-463.

17. Xu YL, Yu Z. Non-linear vibration of cable-damper systems Part II: Application and Verification. *Journal of Sound and Vibration* 1999; **225(3):** 465-481.

18. Johnson EA, Christenson RE, Spencer BF, Jr. Semiactive damping of cables with sag. *Computer-aided Civil and Infrastructure Engineering* 2003; **18(2):** 132-146.

19. Cai CS, Wu WJ, Shi XM. Cable vibration reduction with a hung-on TMD system. Part I: Theoretical study. *Journal of Vibration and Control* 2006; **12(7):** 801-814.

20. Vakakis A. Inducing passive nonlinear energy sinks in vibrating systems. *Journal of Vibration and Acoustics* 2001; **123(3):** 324-332.

21. Vakakis AF, Gendelman OV, Bergman LA, McFarland DM, Kerschen G, Lee YS. *Nonlinear targeted energy transfer in mechanical and structural systems (Volumes I and II)*. Springer Science, New York, New York, USA, 2008.

22. Lee YS, Nucera F, Vakakis AF, McFarland DM, Bergman LA. Periodic orbits, damped transitions and targeted energy transfers in oscillators with vibro-impact attachments. *Physica D: Nonlinear Phenomena* 2009; **238(18):** 1868-1896.

23. Habib G, Detroux T, Viguié R, Kerschen G. Nonlinear generalization of Den Hartog's equal-peak method. *Mechanical Systems and Signal Processing* 2014; **52:** 17-28.

24. Macdonald J. Response amplitudes of non-linear stay cable vibrations (Keynote Lecture), *Proceedings of the Symposium on the Dynamics and Aerodynamics of Cables (SDAC)*, Technical University of Denmark (DTU), Copenhagen, Denmark, 2014.

25. Hoang N, Fujino Y. Multi-mode control performance of nonlinear dampers in stay cable vibrations. *Structural Control and Health Monitoring* 2009; **16(7-8):** 860-868.

26. Alaggio R, Rega G. Characterizing bifurcations and classes of motion in the transition to chaos through 3D-tori of a continuous experimental system in solid mechanics. *Physica D: Nonlinear Phenomena* 2000; **137(1):** 70-93.

27. Srinil N, Rega G, Chucheepsakul S. Three-dimensional non-linear coupling and dynamic tension in the large-amplitude free vibrations of arbitrarily sagged cables. *Journal of Sound and Vibration* 2004; **269(3):** 823-852.

28. Rega G. Nonlinear vibrations of suspended cables—Part I: Modeling and analysis. *Applied Mechanics Reviews* 2004; **57(6):** 443-478.

29. Casciati F, Ubertini F. Nonlinear vibration of shallow cables with semiactive tuned mass damper. *Nonlinear Dynamics* 2008; **53(1-2):** 89-106.

30. Faravelli L, Fuggini C, Ubertini F. Adaptive solution for intelligent cable vibration mitigation. *Advances in Science and Technology* 2009; **56:** 137-146.

31. Faravelli L, Ubertini F. Nonlinear state observation for cable dynamics. *Journal of vibration and Control* 2009; **15(7):** 1049-1077.

32. Xu Y, Yu Z. Vibration of inclined sag cables with oil dampers in cable-stayed bridges. *Journal of Bridge Engineering* 1998; **3(4):** 194-203.

33. Fujino Y, Hoang N. Design formulas for damping of a stay cable with a damper. *Journal of structural engineering* 2008; **134(2):** 269-278.

34. Hoang N, Fujino Y. Combined damping effect of two dampers on a stay cable. *Journal of Bridge Engineering* 2008; **13(3):** 299-303.

35. Hoang N, Fujino Y. Multi-mode control performance of nonlinear dampers in stay cable vibrations. *Structural Control and Health Monitoring* 2009; **16(7-8):** 860-868.

36. Krenk S, Sørensen N. Vibrations of a shallow cable with a viscous damper. *Proceedings Royal Society London A* 2002; **458:** 339-357.

37. Main JA, Jones NP. Evaluation of viscous dampers for stay-cable vibration mitigation. *Journal of Bridge Engineering , ASCE* 2001; **6(6):** 385-397.

38. Caracoglia L, Zuo D. Effectiveness of cable networks of various configurations in suppressing stay-cable vibration. *Engineering Structures* 2009; **31(12):** 2851-2864.

39. Izzi M. *Smorzatori oleodinamici e dispositivi Targeted Energy Transfer per il controllo passivo delle vibrazioni di stralli*. University of Trieste: Trieste, 2013.

40. Giaccu GF, Caracoglia L. Effects of modeling nonlinearity in cross-ties on the dynamics of simplified in-plane cable networks. *Structural Control and Health Monitoring* 2012; **19(3):** 348-369.

41. Chopra AK. *Dynamics of structures*. Prentice Hall New Jersey, 1995.

42. Zuo D, Jones NP. Interpretation of field observations of wind-and rain-wind-induced stay cable vibrations. *Journal of Wind Engineering and Industrial Aerodynamics* 2010; **98(2):** 73-87.

43. Irwin PA. Wind vibrations of cables on cable-stayed bridges, *Proceedings of the Building to Last*, 1997; 383-387.

44. Specification PG. Recommendations for stay cable design, testing and installation. *Post-Tensioning Institute Committee on Cable-Stayed Bridges* 2001.

45. Matsumoto M, Ishizaki H. Stall-type galloping and VIV-initiated galloping of inclined stay cable aerodynamics and its aerodynamic stabilization (Keynote Lecture), *Proceedings of the Symposium on the Dynamics and Aerodynamics of Cables (SDAC)*, Technical University of Denmark (DTU), Copenhagen, Denmark, 2014.

46. Weber F, Feltrin G, Maślanka M, Fobo W, Distl H. Design of viscous dampers targeting multiple cable modes. *Engineering Structures* 2009; **31(11):** 2797-2800.

47. Weber F, Boston C, M. M. Adaptive TMD based on the emulation of positive and negative stiffness with MR damper. *Smart Materials and Structures* 2011; **20(1):** 015012(11).

48. Weber F, Boston C. Clipped viscous damping with negative stiffness for semi-active cable damping. *Smart Materials and Structures* 2011; **20(4):** 045007.

49. Li H, Liu M, Ou J. Negative stiffness characteristics of active and semi-active control systems for stay cables. *Structural Control and Health Monitoring* 2008; **15(2):** 120-142.

NOMENCLATURE

The following symbols were used in this paper:

c	Viscous damper coefficient (kN·m/s)
D	Diameter of cable (m)
F_L, F_R	Transverse force component due to the cable deflection for the *i*th mass (kN)
$\mathbf{f}$	Vector employed to account for the effect of the TET device
f_{j_B}	Interaction force provided by the dashpot
$\mathbf{f}_{\text{nd}}$	Non-dimensional column vector to account for the effect of the TET device
$\mathbf{f}^*$	State-space formulation of the non-dimensional force vector $\mathbf{f}_{\text{nd}}$
i	Mode number
j_B	Degree of freedom at which the TET device is attached to the cable
j_A	Degree of freedom at which the lumped mass is attached to the TET device
$\mathbf{K}$	Stiffness matrix of the cable and elastic support
$\mathbf{K}_1$	$n' \times n'$ indicator-matrix of zeros, ones and minus two
$\mathbf{K}_{\text{nd}}$	Non-dimensional stiffness matrix of the cable and elastic support
k_M	Stiffness coefficient for the power-law elastic spring (kN/m^n)
k_S	Stiffness coefficient for the elastic support (kN/m)
L	Length of cable (m)
L_k	Length of *k*th sub-string (m)
$\mathbf{M}$	Mass matrix of the cable and elastic support
$\mathbf{M}_{\text{cable}}$	Lumped mass matrix of the cable
m_A	Secondary TET mass attached to one end of the dashpot (kg)
M_i	*i*th lumped mass of the discrete model, with $i = \{1, \ldots, n'\}$ (kg)
N_{d}	Non-dimensional scalar parameter
n	Exponent of the power-law elastic stiffness, with $n = \{1, 3, \ldots\}$

n'	Total number of lumped masses along the cable length (degrees of freedom)
$\mathbf{S}$	State-space matrix of the lumped model
$S_c, \hat{S}_c$	Scruton number of the cable
$s(t)$	Transverse vibration of the TET device support
T	Tension in cable (kN)
t	Dimensional time variable (s)
$\mathbf{W}$	State-space vector of the lumped mass model at time τ
χ	Relative displacement between node A and B in the TET device (m)
x_k	Coordinate along the cable chord axis in the *k*th sub-string (m)
$Y_k(x_k)$	Complex mode shape of *k*th cable element
$\mathbf{y},(t),\ddot{\mathbf{y}}(t)$	Vectors of the transverse displacements and accelerations at time t
$y_i, \dot{y}_i, \ddot{y}_i$	Transverse displacement, velocity and acceleration of *i*th mass at time t
$y_k(x_k, t)$	Transverse vibration of *k*th sub-string from equilibrium position
$\mathbf{z}$	Vector of the non-dimensional transverse displacements at time τ
z_i	Non-dimensional transverse displacement of *i*th mass at time
γ	Vibration amplitude of the cable at TET device location (m)
Δ_τ	Peak displacement amplitude at damper location (m) - Nonlinear spring
$\Delta_{\tau,\text{sec}}$	Peak displacement amplitude at damper location (m) - Linear secant spring
Δx	Horizontal spacing between two adjacent lumped masses (m)
$\Delta\lambda_i$	Complex valued frequency shift introduced by the spring and the dashpot
δ	Logarithmic decrement of the structural damping
η	Non-dimensional damper coefficient
$\iota = \sqrt{-1}$	Imaginary unit
$\boldsymbol{\kappa}$	Normalized damper coefficient (non-dimensional parameter group)
λ_i	Non-dimensional complex frequency (eigenvalue) of mode i
μ	Mass per unit length (kg/m)

ν_A	Non-dimensional TET mass coefficient
ξ	Flexibility coefficient of the elastic support
ρ	Air density
τ	Non-dimensional time variable
χ_M	Non-dimensional stiffness coefficient for the power-law elastic spring
χ_S	Non-dimensional stiffness coefficient for the elastic support
ψ	Generalized flexibility of the TET apparatus
$\omega_{0,1}$	Undamped natural frequency of the first mode (rad/s)
ω_{i}	Modulus of the dimensional frequency (eigenvalue) of mode i (rad/s)

Subscripts:

k	Cable segment number ($k=\{1,2\}$)
i	Lumped-mass index (degree of freedom of the discrete model); also used to designate mode number in the universal design curves

List of Figures

Figure 9. Structural damping ratio provided by a H-NL-TET device installed on AS16 stay of the Fred Hartman Bridge (Houston, Texas, USA) when the optimal damping ratio is achieved in the first mode (a) and in the second mode (b).

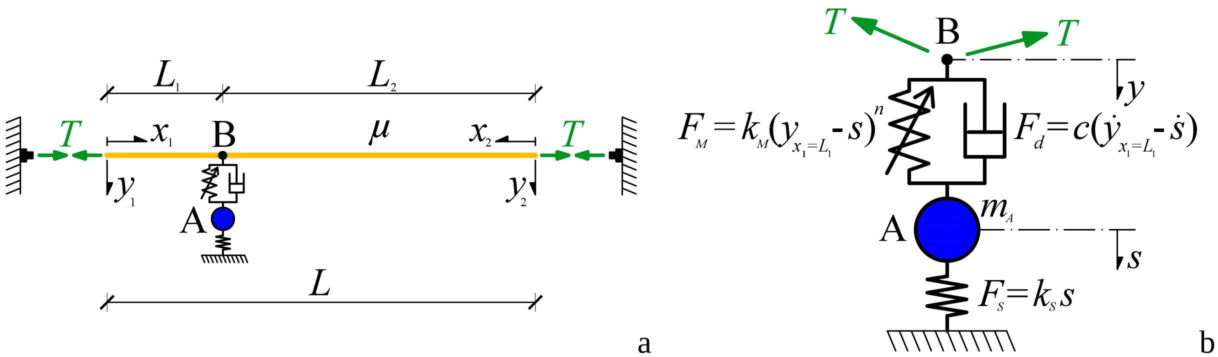

Figure 1.

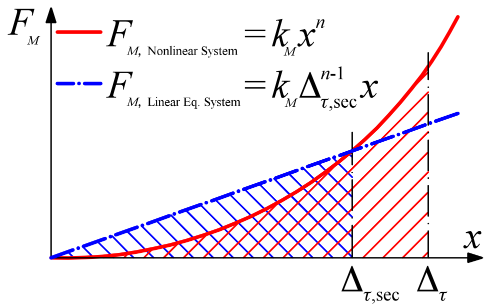
F_M
$F_{M,\ \text{Nonlinear System}} = k_M x^n$
$F_{M,\ \text{Linear Eq. System}} = k_M \Delta_{\tau,\sec}^{n\text{-}1} x$
x
$\Delta_{\tau,\sec}$
Δ_{τ}

Figure 2.

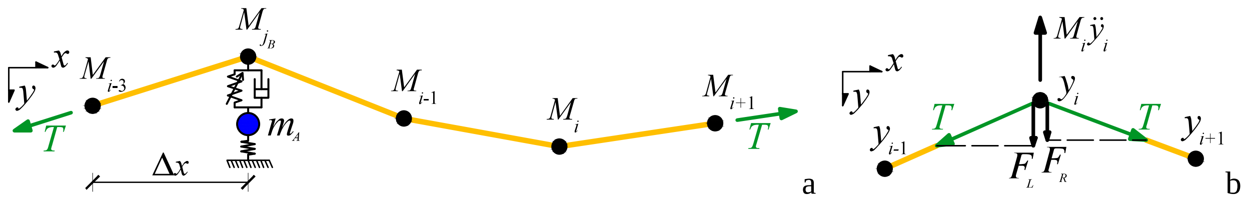

Figure 3.

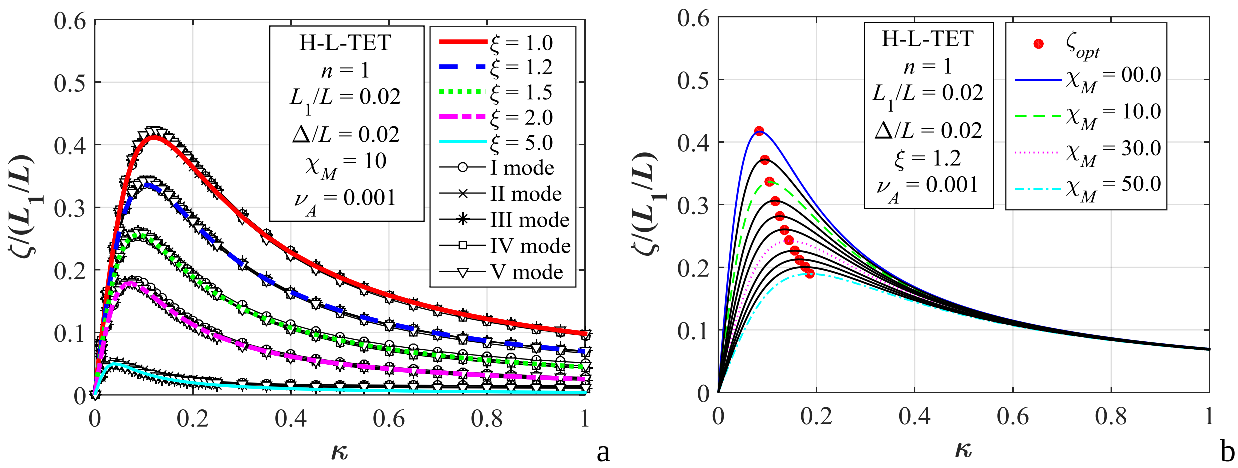

H-L-TET
n = 1
L1/L = 0.02
Δ/L = 0.02
χM = 10
νA = 0.001
ξ = 1.0
ξ = 1.2
ξ = 1.5
ξ = 2.0
ξ = 5.0
I mode
II mode
III mode
IV mode
V mode
ζ/(L1/L)
κ
a
H-L-TET
n = 1
L1/L = 0.02
Δ/L = 0.02
ξ = 1.2
νA = 0.001
ζopt
χM = 00.0
χM = 10.0
χM = 30.0
χM = 50.0
ζ/(L1/L)
κ
b

Figure 4.

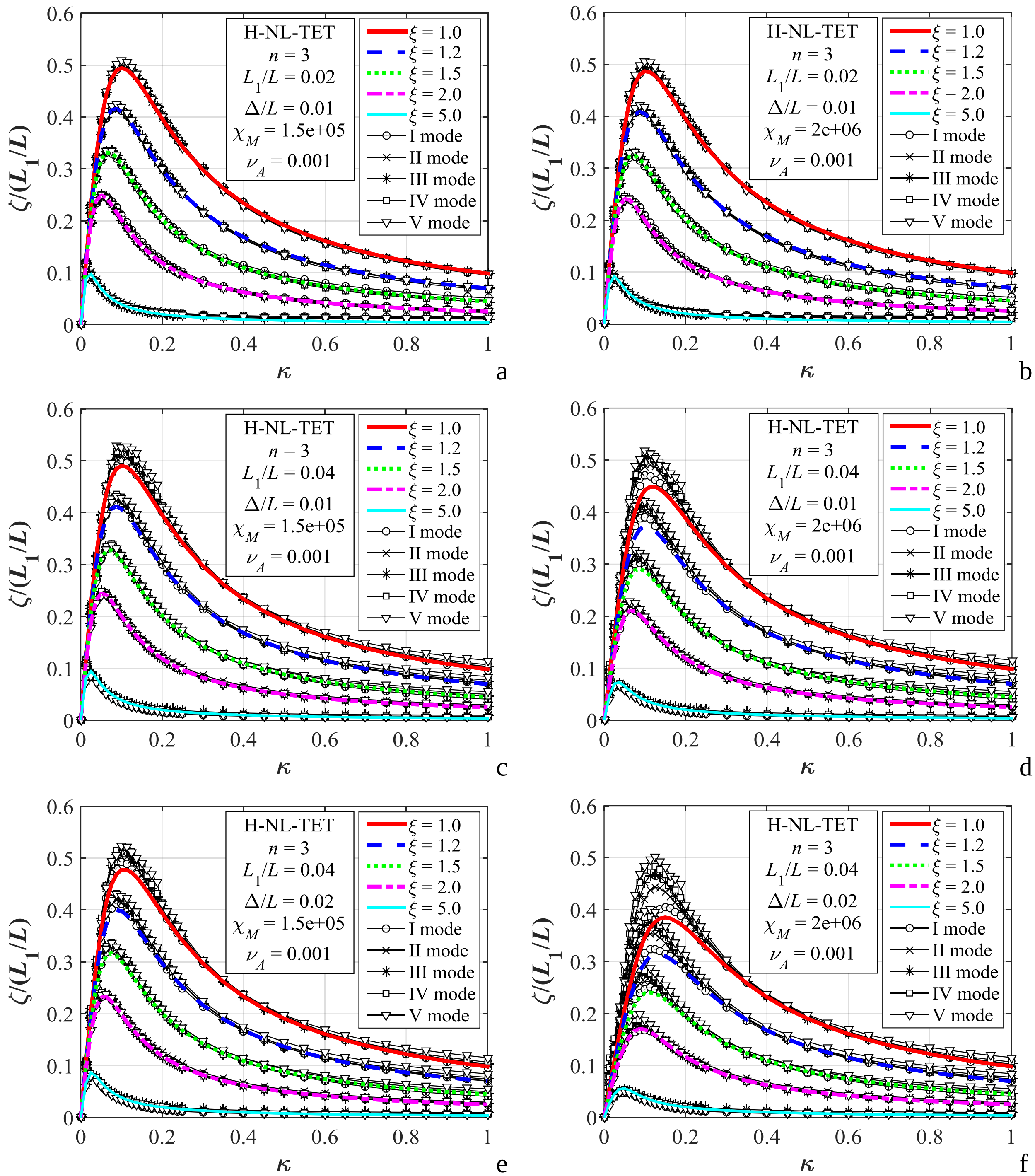
H-NL-TET
n = 3
L1/L = 0.02
Δ/L = 0.01
χM = 1.5e+05
νA = 0.001
ξ = 1.0
ξ = 1.2
ξ = 1.5
ξ = 2.0
ξ = 5.0
I mode
II mode
III mode
IV mode
V mode
ζ/(L1/L)
κ
a
H-NL-TET
n = 3
L1/L = 0.02
Δ/L = 0.01
χM = 2e+06
νA = 0.001
b
H-NL-TET
n = 3
L1/L = 0.04
Δ/L = 0.01
χM = 1.5e+05
νA = 0.001
c
H-NL-TET
n = 3
L1/L = 0.04
Δ/L = 0.01
χM = 2e+06
νA = 0.001
d
H-NL-TET
n = 3
L1/L = 0.04
Δ/L = 0.02
χM = 1.5e+05
νA = 0.001
e
H-NL-TET
n = 3
L1/L = 0.04
Δ/L = 0.02
χM = 2e+06
νA = 0.001
f

Figure 5.

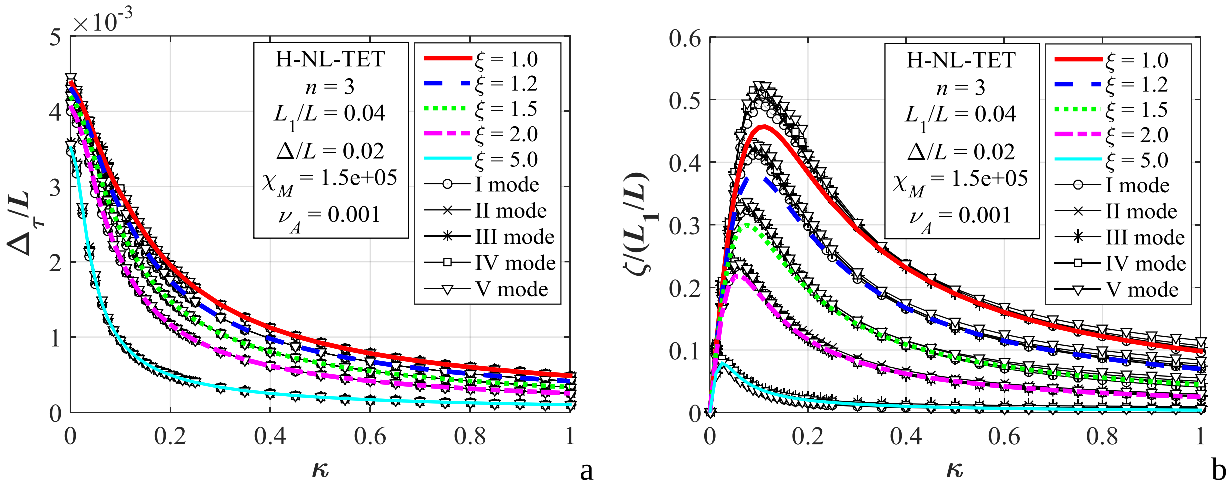

H-NL-TET
n = 3
L1/L = 0.04
Δ/L = 0.02
χM = 1.5e+05
νA = 0.001
ξ = 1.0
ξ = 1.2
ξ = 1.5
ξ = 2.0
ξ = 5.0
I mode
II mode
III mode
IV mode
V mode
Δτ/L
×10-3
κ
a
ζ/(L1/L)
κ
b

Figure 6.

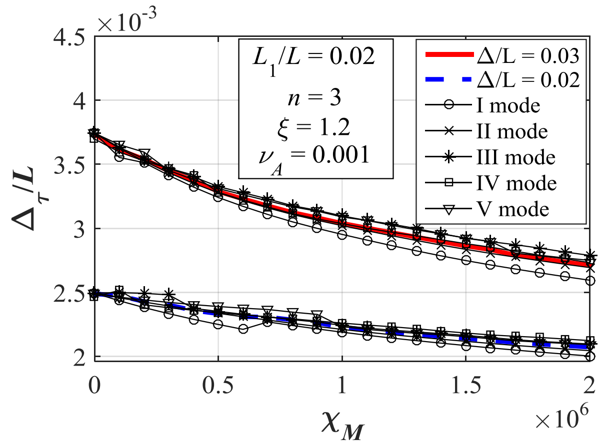
$\times 10^{-3}$
$L_1/L = 0.02$
$n = 3$
$\xi = 1.2$
$\nu_A = 0.001$
$\Delta/L = 0.03$
$\Delta/L = 0.02$
I mode
II mode
III mode
IV mode
V mode
Δ_τ/L
χ_M
$\times 10^{6}$
4.5
4
3.5
3
2.5
2
0
0.5
1
1.5
2

Figure 7.

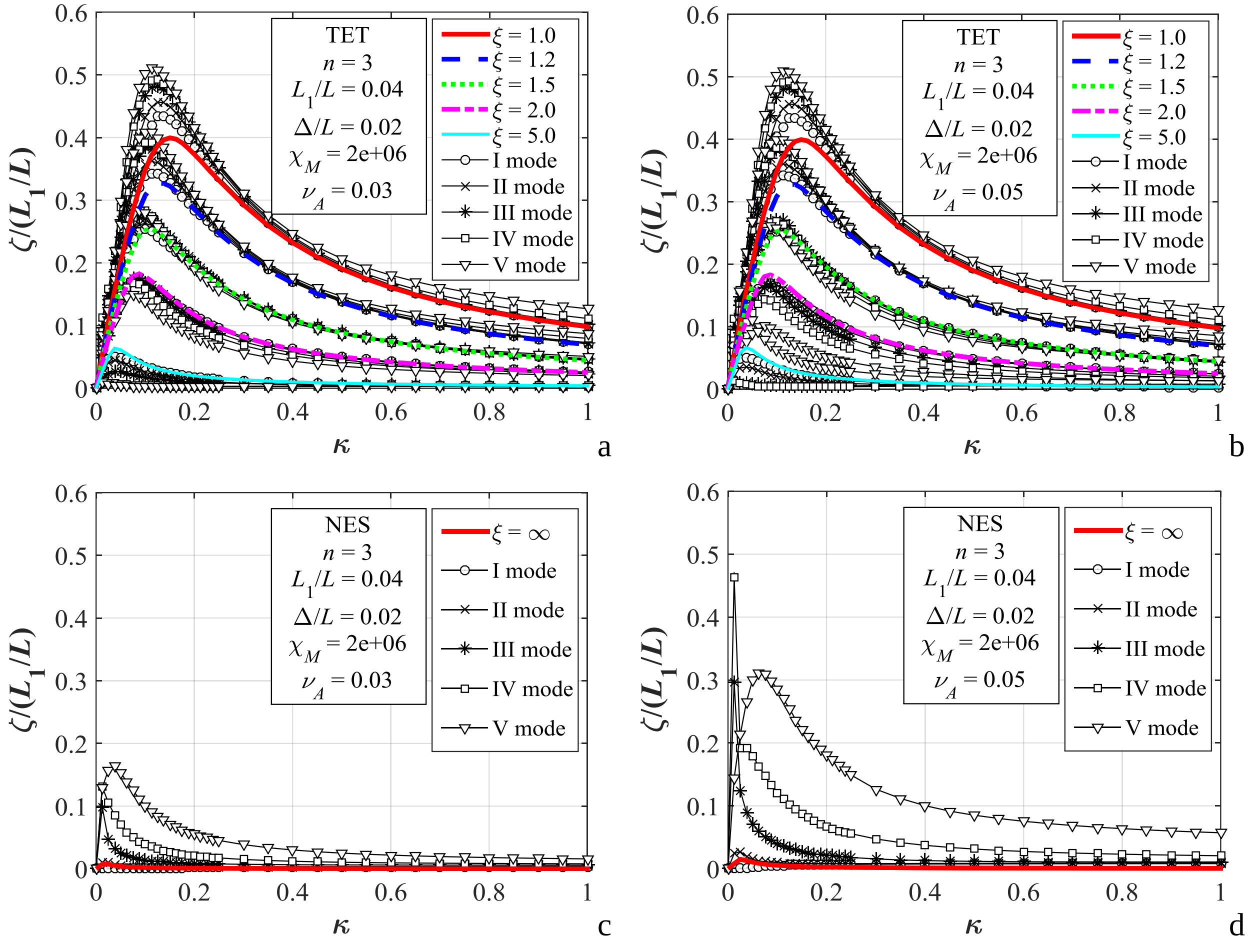
TET
n = 3
L1/L = 0.04
Δ/L = 0.02
χM = 2e+06
νA = 0.03
ξ = 1.0
ξ = 1.2
ξ = 1.5
ξ = 2.0
ξ = 5.0
I mode
II mode
III mode
IV mode
V mode
ζ/(L1/L)
κ
a
TET
n = 3
L1/L = 0.04
Δ/L = 0.02
χM = 2e+06
νA = 0.05
b
NES
n = 3
L1/L = 0.04
Δ/L = 0.02
χM = 2e+06
νA = 0.03
ξ = ∞
c
NES
n = 3
L1/L = 0.04
Δ/L = 0.02
χM = 2e+06
νA = 0.05
d

Figure 8.

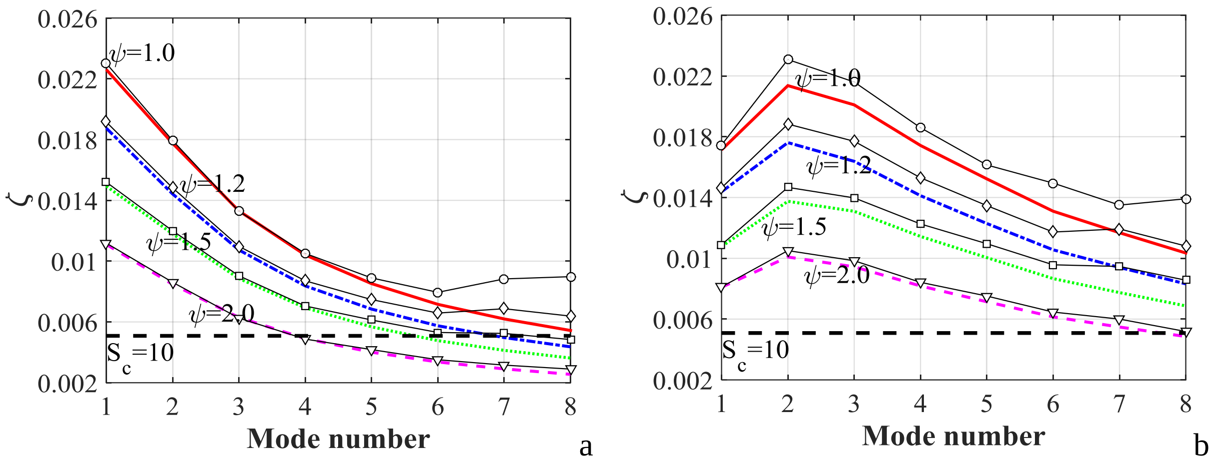

0.026
0.022
0.018
0.014
0.01
0.006
0.002
ζ
ψ=1.0
ψ=1.2
ψ=1.5
ψ=2.0
S c =10
1
2
3
4
5
6
7
8
Mode number
a
b

Figure 9.